PNAS RESEARCH ARTICLE | PHYSIOLOGY

Identification of FSH-regulated and estrous stage–specific transcriptional networks in mouse ovaries

Kathryn Walters[a,b], Amber Baldwin[a,b], Zhenghui Liu[c], Mark Larsen[c], Neelanjan Mukherjee[a,b,1], and T. Rajendra Kumar[c,1]

Edited by Thomas Spencer, University of Missouri, Columbia, MO; received June 14, 2024; accepted January 3, 2025

Follicle-stimulating hormone (FSH) acts by binding to FSHRs expressed on ovarian granulosa cells and produces estradiol. FSH is essential for female fertility because mice lacking FSH (*Fshb KO*) are anestrous and infertile. Although several in vitro cell culture and ex vivo approaches combined with pharmacological hormone treatment were used to identify FSH-regulated genes, how FSH orchestrates ovarian gene networks in vivo has not been investigated. Whether FSH-regulated genes display estrous stage–specific expression changes has also not been studied. Here, we functionally rescued *Fshb* null mice with a gonadotrope-targeted *HFSHB* transgene and performed RNA-Seq analysis on ovarian RNAs obtained from FSH-intact (*WT*), FSH-deficient (*Fshb KO*), and FSH-rescue (*HFSHB*$^{+}$ rescue) mice. By comparing *WT* vs. *Fshb KO* and *Fshb KO* vs. *HFSHB*$^{+}$ rescue ovarian gene expression datasets, we identified FSH-responsive genes in vivo. Cross interrogation of these datasets further allowed us to identify several transcription factors (TFs) and RNA-binding proteins specific to FSH-regulated genes. In an independent set of experiments, we performed RNA-Seq analysis on ovarian RNAs from mice in diestrous (DE), proestrous (PE), and estrous (E) and identified estrous stage–specific ovarian gene expression patterns. Interestingly, many of the FSH-regulated TFs themselves were estrous-stage specifically expressed. We found that ESR2 and GATA6, two known FSH-responsive TFs, and their target genes are reciprocally regulated with distinct patterns of expression in estrous stages. Together, our in vivo models and RNA-Seq analyses identify FSH-regulated ovarian genes in specific estrous stages that are under transcriptional and posttranscriptional control.

FSH | ovary | estrus cycles | transcription factors | RNA-binding proteins

Significance

Despite decades of work on follicle-stimulating hormone (FSH) action in ovaries, how FSH regulates transcriptional networks in vivo has not been studied. Here, using RNA-Seq analysis on ovaries obtained from mice with intact FSH, no FSH, or FSH rescue, we have identified FSH-responsive genes that are estrous specifically regulated in vivo. Our studies may eventually allow us to identify potential targets for fertility enhancement or blockade in women.

Follicle-stimulating hormone (FSH) is a heterodimeric pituitary glycoprotein synthesized in gonadotropes (1–3). It consists of a common α-subunit that is also present in other pituitary glycoprotein hormones and a hormone-specific FSHβ-subunit. Only FSH heterodimer is secreted from the pituitary and is biologically active (1–3). FSH binds to FSH-receptors expressed on ovarian granulosa cells and regulates granulosa cell proliferation and differentiation. Ovarian aromatase expression is exquisitely sensitive to FSH signaling and this enzyme is critical for estrogen production from granulosa cells. Female mice lacking *Fshb* (*Fshb*$^{-/-}$) and hence FSH dimer are infertile because of preantral stage block in ovarian folliculogenesis (4). These mutant female mice do not cycle, are anovulatory, and demonstrate suppressed aromatase in ovaries. *Fshb*$^{-/-}$ mutant mice retain FSH responsiveness and thus can be rescued either genetically by gonadotrope-targeted expression of a human *FSHB* transgene (5, 6) or pharmacologically by supplementation of exogenous recombinant human FSH/FSH analogs (7).

Estrous cycle in mice is characterized by changes in production of estrogen which in turn acts on ovarian cells to regulate both cell proliferation and folliculogenesis (8, 9). Estrogen binds to ESR1 and ESR2, the two classical nuclear receptors that are differentially expressed in specific cell types within the ovary (10–12). Although several biochemical and genetic mouse models delineated the in vivo roles of ESR1 and ESR2 in the ovary (11), the estrogen-regulated gene networks as a function of estrous stage are not known. Similarly, whether FSH-regulated gene networks are also under the regulation of estrogen action in the mouse ovary are not known.

In this manuscript, we have taken advantage of our well-characterized *Fshb* null mice that are genetically rescued with a *HFSHB* transgene (4, 6) and identified FSH-regulated gene networks in vivo in ovaries. Additionally, we have captured the estrous stage–specific gene expression patterns using RNA-Seq and compared the gene networks regulated by FSH in each of the estrous stages. We identified several transcription factors (TFs) downstream of FSH and found their target gene clusters are estrous stage–specifically regulated. We further found that many of the FSH-responsive target genes in these clusters contain

Author affiliations: [a]Department of Biochemistry and Molecular Genetics, University of Colorado Anschutz Medical Campus, Aurora, CO 80045; [b]RNA Bioscience Initiative, University of Colorado Anschutz Medical Campus, Aurora, CO 80045; and [c]Division of Reproductive Sciences, Department of Obstetrics and Gynecology, University of Colorado Anschutz Medical Campus, Aurora, CO 80045

Author contributions: N.M. and T.R.K. designed research; K.W., A.B., Z.L., M.L., and T.R.K. performed research; K.W., Z.L., N.M., and T.R.K. analyzed data; N.M. and T.R.K. obtained funding; and N.M. and T.R.K. wrote the paper.

The authors declare no competing interest.

This article is a PNAS Direct Submission.

[1]To whom correspondence may be addressed. Email: neelanjan.mukherjee@cuanschutz.edu or raj.kumar@cuanschutz.edu.

This article contains supporting information online at https://www.pnas.org/lookup/suppl/doi:10.1073/pnas.2411977122/-/DCSupplemental.

Published February 10, 2025.

ESR and other TF binding motifs. Our studies provide insights into FSH regulated TFs and estrous stage–specific target gene networks in the mouse ovary.

Results

Transcriptomic Changes in Mouse Ovaries in the Absence of FSH. Adult female *Fshb*$^{-/-}$ mice at 9 wk of age showed small ovaries and folliculogenesis block at preantral stage lacking corpora lutea (Fig. 1*A*) indicating these null mice are anovulatory, as described (6, 13). To understand the molecular basis of ovarian defects in the absence of FSH at the transcriptomic level, we performed poly(A) RNA-seq on ovaries obtained from *Fshb*$^{-/-}$ (*Fshb KO*), *Fshb*$^{+/-}$ (*Fshb HET*), and *Fshb*$^{+/+}$ (*Fshb WT*) mouse littermates. As expected (14), *Fshb KO* samples had substantially different gene expression profiles compared to either *Fshb*$^{+/-}$ or *Fshb*$^{+/+}$ samples (Fig. 1*B* and *SI Appendix*, Fig. S1 *A* and *B*). Because the gene expression profiles in ovaries of *Fshb*$^{+/+}$ and *Fshb*$^{+/-}$ were indistinguishable, we focused on comparing gene expression profiles of *Fshb*$^{-/-}$ and *Fshb*$^{+/+}$ ovaries. We identified 982 differentially expressed genes (adjusted $P < 0.05$ and greater than twofold mean expression difference) between *Fshb KO* and *Fshb WT* ovaries (Dataset S1). Of these, 533 were FSH-activated genes, which had higher expression in *WT* than *KO* and 449 were FSH-repressed genes, which had lower expression in *WT* than *KO* (Fig. 1*B*). First, we compared individual genes that were previously known to be FSH-regulated in mouse ovaries by microarrays (14). Indeed, all genes exhibited the expected response of up- or downregulated in the ovaries of *Fshb KO* compared to *WT* in the RNA-Seq data (*SI Appendix*, Fig. S1*C*) as well as qPCR validation (Fig. 1*C*). Furthermore, genes that were activated by FSH in ex vivo rat granulosa cells (15) were also strongly enriched for being FSH-activated genes (adj. *P*-value = 0.004699) (Fig. 1*D*). Finally, we identified pathways enriched in FSH-activated genes and FSH-repressed genes using GSEA (16). Inflammation and cholesterol homeostasis were among the FSH-activated pathways and MYC targets and mitotic cell cycle (G2/M) pathways were among the FSH-repressed pathways (*SI Appendix*, Fig. S1*D* and Dataset S2) consistent with known FSH roles in granulosa cell proliferation and preparing follicles for ovulation and subsequent corpus luteum formation (9, 17–19). Taken together, our data were consistent with previously published data, and we identified FSH-regulated pathways in mouse ovaries.

Transcriptomic Changes in Ovaries of *Fshb KO* Mice Genetically Rescued with a Gonadotrope-Targeted *HFSHB* Transgene. Phenotypic defects in ovarian folliculogenesis in *Fshb*$^{-/-}$ mice were genetically rescued by a gonadotrope-targeted human *FSHB* (*HFSHB*) transgene, which is consistent with our previous rescue experiments (5, 6). These mice exhibited estrous cycles and ovarian histology shows multiple stages of growing follicles including corporal lutea indistinguishable from those seen in ovaries of *WT* control mice (Fig. 2*A*). However, there has not been a transcriptome-wide and unbiased examination of molecular phenotypes in these rescue mice. Therefore, we performed poly(A) RNA-seq on ovaries from *Fshb KO* and *Fshb*$^{-/-}$ *HFSHB*$^{+}$ (*HFSHB* rescue) mouse littermates. *Fshb KO* ovary samples had clearly distinguishable gene expression profiles from *HFSHB* rescue ovary samples (Fig. 2*B* and *SI Appendix*, Fig. S2 *A* and *B*). Overall, we identified 1,179 differentially expressed genes (adjusted $P < 0.05$ and greater than twofold mean expression difference) between ovaries from *Fshb KO* and *HFSHB* rescue mice (Dataset S1). Of these, 535 were FSH-activated genes, which had higher expression in *HFSHB* rescue than *Fshb KO* and 644 were FSH-repressed genes, which had lower expression in *HFSHB* rescue than *Fshb*

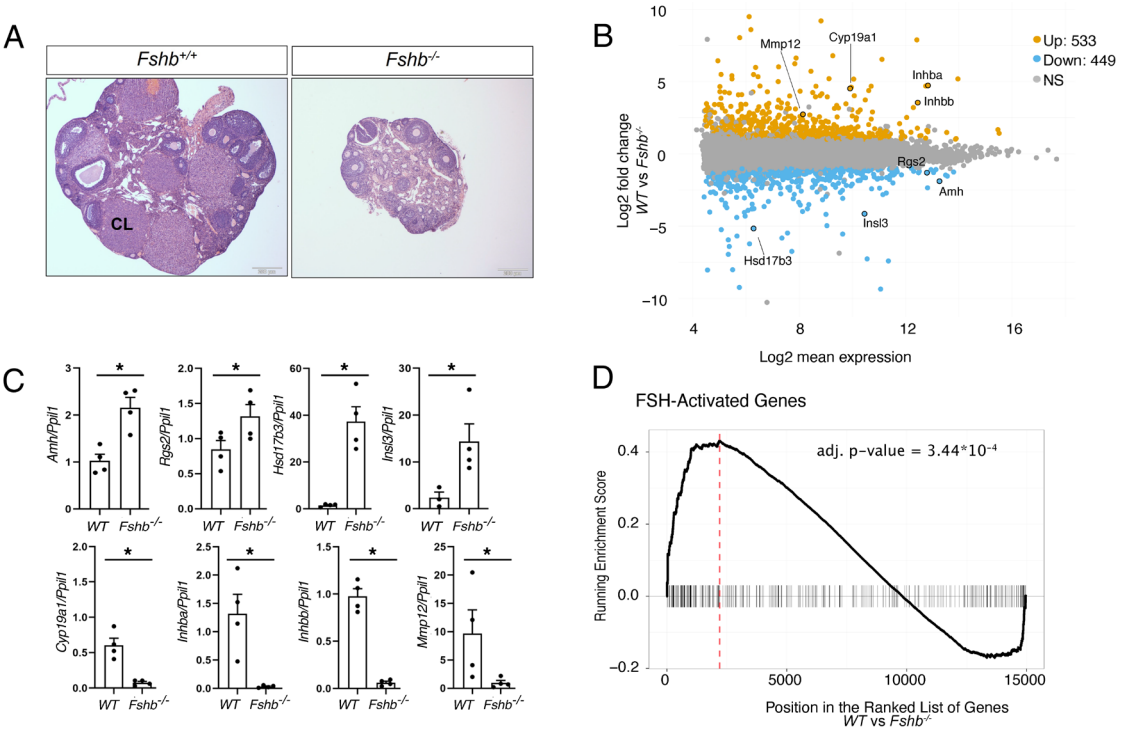

Fig. 1. Transcriptomic changes in *Fshb KO* mouse ovaries. (*A*) Histology of an adult wild-type (*WT*) mouse ovary *Fshb*$^{+/+}$ (*Left*) shows multiple stages of follicles including corpus luteum whereas folliculogenesis is arrested in ovarian section obtained from age-matched *Fshb* knockout *Fshb*$^{-/-}$ (*Right*) mouse, which mostly shows immature follicles. (Scale bar, 200 μm.) (*B*) MA plot of the log2 fold change in gene expression between *WT* and *Fshb*$^{-/-}$ transcripts (*y*-axis) and the log2 of mean of gene expression (*y*-axis). Significant (*P*adj < 0.05, log2FC > |1|) genes are indicated in orange (upregulated), blue (downregulated), and gray (not significant). (*C*) Taqman qPCR analysis on ovarian RNA shows the normalized qPCR expression of individual transcripts in *WT* and *Fshb*$^{-/-}$ mouse ovaries. Triplicate cDNA samples form ovaries of at least four adult female mice per group were analyzed; *denotes $P < 0.05$ by Student's *T* test. (*D*) GSEA of ranked expression changes FSH-activated genes in ovaries of *WT* vs. *Fshb*$^{-/-}$ ovaries.

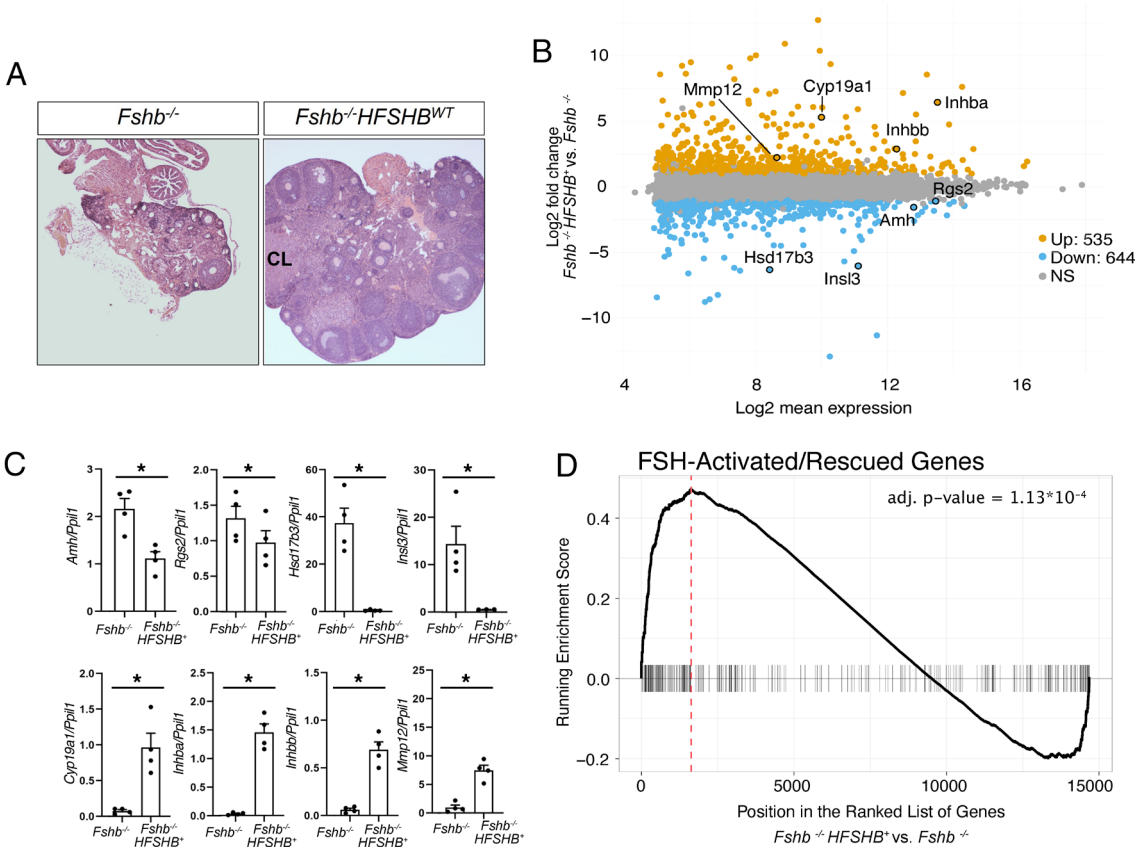

Fig. 2. Transcriptomic changes in *HFSHB*$^{+}$ *rescue* mouse ovaries. (*A*) Genetic rescue of *Fshb*$^{-/-}$ mice with a gonadotrope-targeted *HFSHB* transgene. Histological analysis indicates that folliculogenesis resumes with multiple stages of follicles present in ovarian section of rescued mouse ovary, *Fshb*$^{-/-}$ *HFSHB*$^{+}$ (*Right*) compared to ovarian section obtained form *Fshb*$^{-/-}$ ovary (*Left*). (Scale bar, 200 μm.) (*B*) MA plot shows the log2 fold change in gene expression between *Fshb*$^{-/-}$ *HFSHB*$^{+}$ and *Fshb*$^{-/-}$ (*y*-axis) transcripts and log2 of mean gene expression (*x*-axis). Significant (*P*adj < 0.05, log2FC > |1|) genes indicated in orange (upregulated), blue (downregulated), and gray (not significant). (*C*) Taqman qPCR assays (Bar plots) depict the normalized qPCR expression of individual transcripts in *Fshb*$^{-/-}$ and *Fshb*$^{-/-}$ *HFSHB*$^{+}$ (rescue) mouse ovaries. Note the clear and opposite patterns of expression of marker genes compared to those in panel Fig. 1*C*. For qPCR analysis, triplicate cDNA samples form ovaries of at least four adult female mice per group were analyzed; * denotes $P < 0.05$ by Student's *T* test. (*D*) GSEA of FSH-activated/rescued genes in ovaries of *Fshb*$^{-/-}$ *HFSHB*$^{+}$ vs. *Fshb*$^{-/-}$ mice.

KO (Fig. 2*B*). Again, we examined individual genes known to be differentially regulated by FSH (14) and confirmed that they exhibited the expected response in ovaries of *Fshb KO* compared to *HFSHB* rescue mice in both the RNA-Seq data (*SI Appendix*, Fig. S2*C*) and by qPCR validation (Fig. 2*C*). As expected, genes that were activated by FSH in ex vivo rat granulosa cells (15) were strongly enriched for being FSH-activated genes (adj. *P*-value = 0.000113) (Fig. 2*D* and Dataset S2). As in the *Fshb KO* vs. *Fshb WT* comparison, inflammation and cholesterols homeostasis pathways were among the FSH-activated pathways and MYC and E2F target pathways were among the FSH-repressed pathways (*SI Appendix*, Fig. S2*D* and Dataset S2). These data indicate that genetic rescue with *HFSHB* on the *Fshb KO* genetic background produces histological and transcriptomic phenotypes essentially indistinguishable from those seen in *Fshb WT* mouse ovaries.

Integrating Transcriptomic Signatures of *Fshb KO* and *HFSHB* Transgene Rescue Models to Define *Fshb*-Regulated Genes in Mouse Ovaries. To identify FSH-regulated genes and given the slight discrepancy in the number of differentially expressed genes caused by *Fshb KO* and *HFSB* rescue, we conducted a detailed comparison of the FSH-activated and FSH-repressed genes identified in the two different mouse models. FSH-activated and FSH-repressed genes identified by the two different models had statistically significant overlap (Fig. 3*A*) and were nearly 50-fold more likely to overlap than chance (46× and 49×, respectively). Furthermore, there was a very strong correlation in the magnitude and direction of expression changes for the union of all genes identified as FSH-activated and repressed from both mouse models (Fig. 3*B*). Next, we tested whether FSH-activated and repressed gene sets defined from the *HFSHB* rescue model were enriched or depleted in the *Fshb* KO model. The vast majority of FSH-activated genes were upregulated in the *Fshb KO* compared to *Fshb WT* and, the vast majority of FSH-repressed genes were downregulated in the *Fshb KO* compared to *Fshb WT* (*SI Appendix*, Fig. S3*A*). The same pattern holds consistently when the gene sets defined using the *Fshb KO* model were queried for enrichment or depletion in the *HFSHB* rescue model (*SI Appendix*, Fig. S3*B*). Beyond experimentally defined FSH-regulated genes, we also found that enrichment/depletion of the same pathways were completely concordant in both mouse models (*SI Appendix*, Fig. S3 *C* and *D*, and Dataset S2). In summary, both models, i.e., *WT* vs. *Fshb KO* and *Fshb KO* vs. *HFSHB* rescue, essentially identified essentially the same sets of genes. Thus, we defined the FSH-regulated genes in mouse ovaries as the union of the differentially expressed genes in the two genetic models (Dataset S1).

Transcriptional and Posttranscriptional Regulation of FSH-Responsive Genes. We next set out to identify gene regulatory networks downstream of FSH signaling that orchestrate the FSH-activated and -repressed genes. It is likely that FSH signaling in ovarian granulosa cells is coupled to cascade of TFs that ultimately regulate sets of FSH-responsive genes further downstream. Therefore, we first examined promoter sequences within the

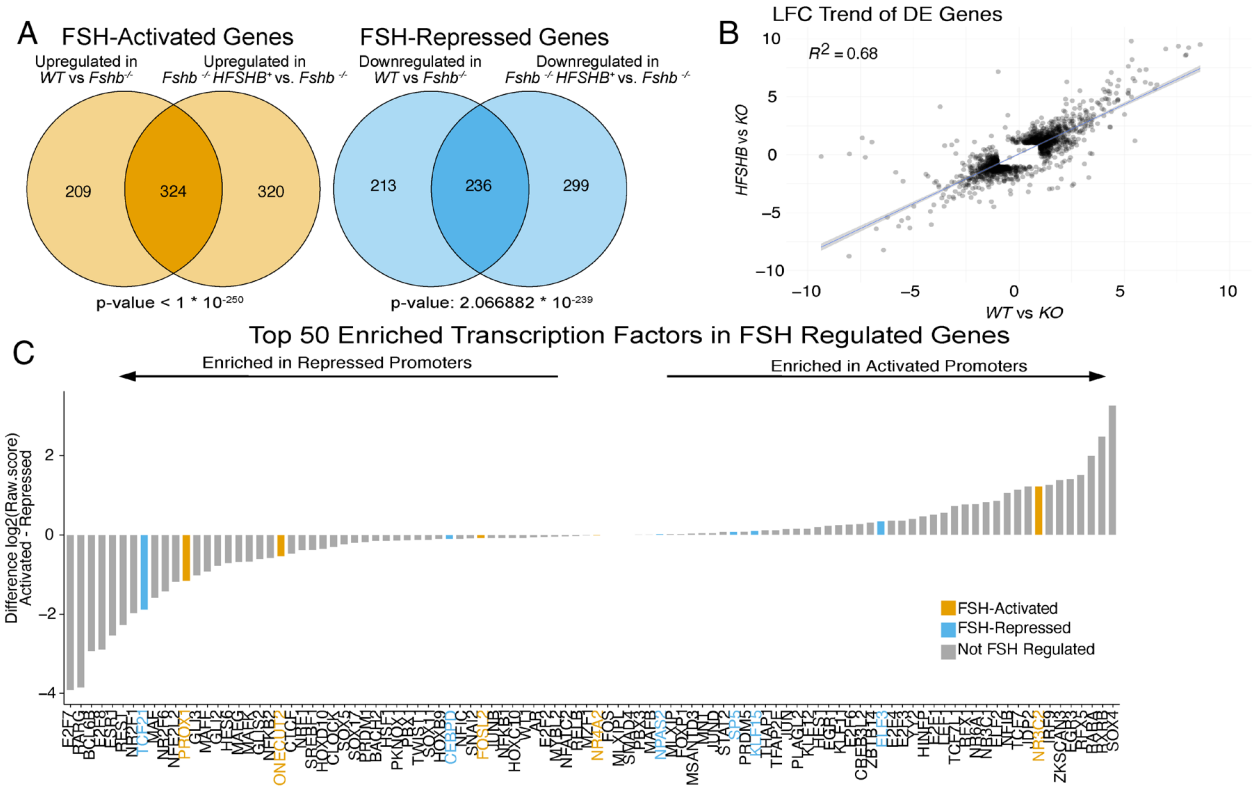

Fig. 3. Identification of FSH-regulated genes. (*A*) Venn diagram of the overlap of FSH-activated (*Left*) or FSH-repressed genes (*Right*) from the *WT* vs. *Fshb*$^{-/-}$ and *Fshb*$^{-/-}$ vs. *Fshb*$^{-/-}$ *HFSHB*$^{+}$ experimental datasets. (*B*) Scatterplot shows the correlation between differentially expressed genes in *WT* vs. *Fshb*$^{-/-}$ and *Fshb*$^{-/-}$ vs. *Fshb*$^{-/-}$ *HFSHB*$^{+}$ experimental comparisons. (*C*) Topmost 50 TFs with motifs enriched, as determined by the log2 difference in enrichment raw score between activated and repressed categories, in FSH-repressed (*Left*) or FSH-activated (*Right*) promoters. Bars highlighted orange (activated) or blue (repressed) indicate direct FSH regulation of the indicated TF.

FSH-activated and repressed gene sets where relevant TFs might bind. Since FSH is required for estrogen production via cAMP-PKA pathway and thus indirectly regulates estrogen receptor (ER)–controlled gene networks, we calculated the enrichment of ESR1 and ESR2 binding motifs in the promoters of FSH-activated and repressed genes. ESR1, ESR2, and CREB1 recognition motifs were strongly enriched in promoters of both FSH-activated and repressed genes (*SI Appendix*, Fig. S3*E*), which is consistent with ESR2 expression in granulosa cells within the ovarian follicles where FSH acts by binding to FSHRs (8, 9, 17, 18). Some of the DEGs may be expressed in theca cells due to the indirect effect of *Fshb* deletion, particularly those that contain ESR1 binding motifs because ESR1 is expressed in theca cells. Given our ability to identify known transcriptional regulators using this enrichment strategy, we expanded the analysis and identified 284 different TF motifs with statistically significant enrichment in the promoters of FSH-activated and/or FSH-repressed genes of which the top 50 contained several known and TFs (Dataset S3).

We then focused on the TFs that exhibited the largest difference in motif enrichment between activated promoter sequences and repressed promoter sequences (Fig. 3*C*). Interestingly, we found that 7 FSH-activated, 6 FSH-repressed TFs within this group were themselves FSH-activated or repressed. We found that ESR1 was an FSH-activated gene with higher motif enrichment in repressed promoters (*SI Appendix*, Fig. S3*E*). Together, our analyses identified FSH-regulated TF regulatory networks in mouse ovaries.

Posttranscriptional regulation plays a major role in mRNA stability and turnover and may be critical for FSH-regulated processes within the ovarian follicle. RNA-binding proteins (RBP) are key regulators of RNA decay and control target gene expression levels (20, 21). Therefore, analogous to the TF-promoter analysis, we searched for RBP regulatory motifs enriched in the 3′ untranslated region (3′ UTR) of FSH-activated and/or FSH-repressed mRNAs. We identified 27 RBP motifs, of which 9 were preferentially enriched in 3′ UTRs of FSH-activated genes, while 18 were enriched in 3′ UTRs of FSH-repressed genes (*SI Appendix*, Fig. S3*F*). We found that FSH-repressed 3′ UTRs were enriched for motifs corresponding to Musashi-1 (Msi1); indeed, the Musashi family of RBPs are required for proper ovarian follicle development (22). None of the other RBPs that preferentially target FSH-activated 3′ UTRs had any known role in ovarian function, which is not surprising given they have never been investigated. PCBP1 and PCBP2 motifs were both enriched in FSH-repressed 3′ UTRs (*SI Appendix*, Fig. S3*F*). Thus, we identified many RBPs that may represent important in vivo regulators of FSH-regulated gene networks in mouse ovaries.

FSH-Regulated Gene Expression Dynamics During Mouse Estrous Cycle. FSH regulates aromatase gene expression and estradiol production from ovarian granulosa cells and thus is one of the master trophic regulators of the estrous cycle (1, 9, 23). However, estrous stage–dependent in vivo expression dynamics of FSH-regulated genes is not known. To address this, we performed poly(A) RNA-seq on quadruplicate ovarian RNA samples obtained from female mice at the diestrous (DE), proestrous (PE), and estrous (E) stages (Fig. 4*A*). As expected, DE and PE stage global expression profiles were more similar to each other than they were to E stage and anestrous *Fshb KO* ovaries (Fig. 4*B* and *SI Appendix*, Fig. S4*A*). We then examined estrous stage–specific changes in the FSH-responsive genes we defined above. We clustered FSH-regulated genes based on their stage-specific expression and identified six unique patterns of expression changes through the estrous cycle (Fig. 4*B*). All these clusters exhibited expression dynamics throughout the estrous cycle

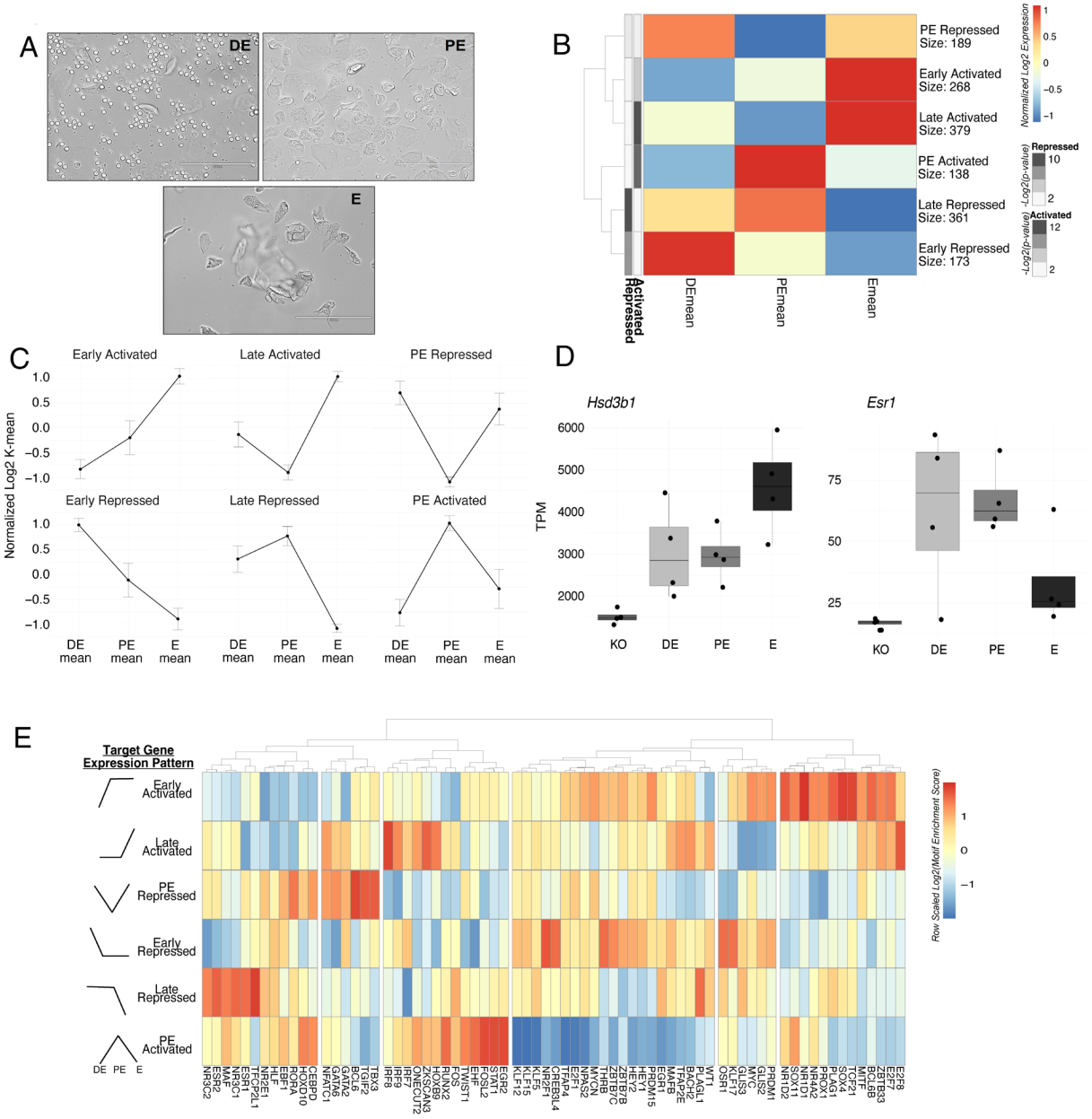

Fig. 4. FSH-regulated gene expression changes during mouse estrous cycle. (*A*) Vaginal cytology of cycling female mice in diestrous (DE), proestrous (PE), and estrous (E) stages. (*B*) k-means clustered heatmap shows the expression changes of FSH-regulated genes during each stage of the estrous cycle. FSH-repressed and FSH-activated gene enrichment in each cluster shown along the *y*-axis. (*C*) Line graphs of the normalized log2 k-mean value for each cluster at each indicated estrous stage. (*D*) TPM normalized expression of individual transcripts shown in *Fshb*$^{-/-}$ mice or mice staged in DE, PE, or E stage of estrous cycle. n = 4. (*E*) Heatmap of TF motif enrichment in the promoters of genes belonging to each of the six estrous cycle clusters. TFs included are those that are FSH-regulated at the RNA level in at least one experiment (*P*. adj < 0.05 & lfc > |0.5 |).

(Fig. 4*C*), i.e., we could not identify a pattern associated with no change in expression for the FSH-regulated genes. Furthermore, the late activated genes were the most enriched for being FSH-activated (*Hsd3b1*), while the late repressed genes were the most enriched for being FSH repressed (*Esr1*) (Fig. 4*D*), consistent with their known physiological functions, such as steroidogenesis and granulosa cell differentiation, respectively. We further found that ESR1 and ESR2 motifs were preferentially enriched specifically in the promoters of genes in the late repressed cluster (*SI Appendix*, Fig. S4*C*). We expanded this cluster analysis to all TFs and their estrous cycle patterns (Fig. 4*E* and *SI Appendix*, Fig. S4*D*) and found that specific subsets of TF motifs were enriched estrous stage specifically (Fig. 4*E*). Collectively, these data indicate that FSH orchestrates cascades of TFs which regulate genes with dynamic expression pattern specific to each stage of the estrous cycle.

FSH binds FSHRs exclusively expressed on ovarian granulosa cells and regulates granulosa cell proliferation and differentiation (9, 17, 18, 23). To validate our bulk RNA-seq data to granulosa cell transcriptional networks, we analyzed published ovarian single-cell RNA-seq dataset that had identified many different cell populations (*SI Appendix*, Fig. S5*A*) (24) and focused on the 499 genes specifically enriched in granulosa cells. By mapping their gene expression changes throughout the mouse estrous cycle, we grouped them into six distinct clusters (Fig. 5*A*). We then searched for TF motifs enriched in these clusters and found 13 TFs that are FSH-regulated and granulosa cell–enriched (Fig. 5*B* and *SI Appendix*, Fig. S5*B*). Two known FSH-regulated and granulosa cell–enriched TFs *Esr2* and *Gata6* (Fig. 5*C*) and their corresponding target genes were further analyzed and showed estrous stage–specific dynamic expression pattern (Fig. 5*D*). Computational analysis further identified ESR2

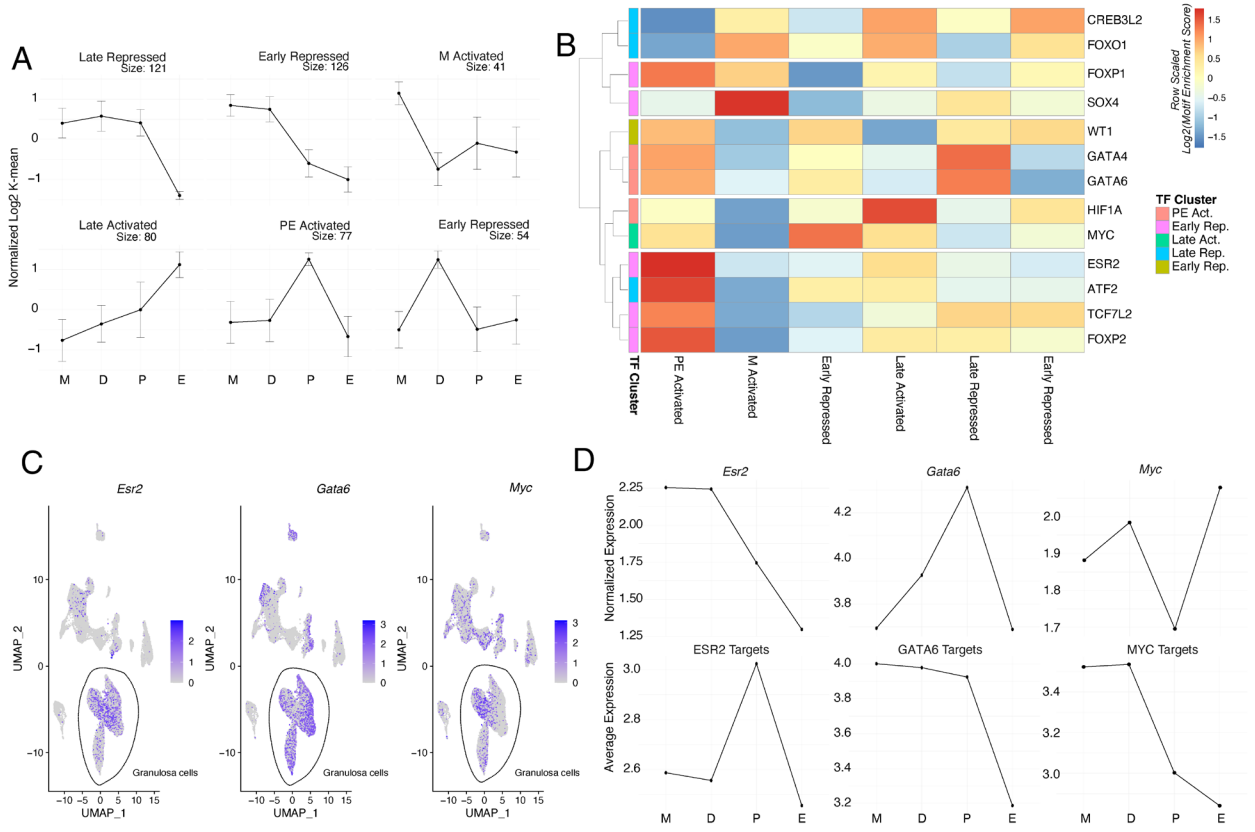

Fig. 5. Characterization of trans-acting regulatory dynamics of FSH-regulated genes during mouse estrous cycle. (*A*) Line graphs of the normalized log2 k-mean value for each cluster throughout each stage of the mouse estrous cycle (data analyzed from ref. 24). (*B*) Heatmap shows motif enrichment in the promoters of genes belonging to granulosa cell-specific genes sorted by mouse estrous stage cluster identity. TFs shown have granulosa cell-specific expression and have motifs enriched in cycling FSH-regulated genes. Colored annotation indicates which granulosa cluster each TF is found in based on its expression. (*C*) UMAP projection depicting cell-specific expression for *Esr2, Gata6,* and *Myc*. Dotted lines indicate subpopulations of granulosa cells. (*D*) Line graphs show normalized expression levels of *Esr2* or *Gata6* or *Myc* and the average normalized expression levels of transcripts containing ESR2-, GATA6-, or MYC-binding sites throughout the estrous cycle.

and GATA6 binding sites in promoters of their corresponding target genes (*SI Appendix*, Fig. S5*C*). In addition, we found that MYC is highly enriched in granulosa cells and both *Myc* and MYC-targets also show estrous stage–specific expression pattern (Fig. 5 *C* and *D*). Thus, our data obtained with bulk RNA-seq closely aligns with the published granulosa cell –enriched single-cell RNA-seq data (24) and further validates our computational analysis.

Discussion

FSH regulates ovarian granulosa cell proliferation and differentiation and female fertility. However, the molecular basis for these critical processes in ovarian development is unknown. Female mice lacking *Fshb* (and hence FSH) are anestrous and infertile because of arrested folliculogenesis at the preantral stage (4, 6). Our genetic approach to rescue *Fshb* null mice with a *HFSHB*+ transgene appropriately expressed and regulated indistinguishably to *Fshb* in pituitaries of normal mice provided a clean physiological system without the need for culturing granulosa cells and exogenous treatment of these cells with FSH in vitro (25).

Bulk RNA–Seq pairwise analysis on ovaries obtained from adult WT (*Ctrl*) vs. *Fshb KO* and *Fshb KO* vs. *HFSHB*+ rescue mice allowed us to identify FSH-regulated gene networks in vivo. Integration of overlapping data on differentially regulated ovarian genes under three different physiological conditions (normal FSH, no FSH, and FSH rescue) led us to identify FSH-regulated genes. Some of the RNA-Seq data may represent differentially expressed genes because of the lack of advance stage follicles between control vs. $Fshb^{-/-}$ ovaries. However, follicles up to secondary (preantral) stage are common and the cellular composition as assessed by marker genes remains the same between these two genotypes (*SI Appendix*, Fig. S6). We have compared two other published datasets of FSH-responsive genes (14, 26) and identified remarkable similarities among those and our RNA-Seq datasets (*SI Appendix*, Fig. S7). The more precise way to identify true bona fide FSH-responsive genes would be to temporally delete *Fshb* or *Fshr* in the ovaries of adult mice and perform RNA-Seq analysis. However, one limitation with the temporal deletion models is that inefficient recombination efficiency at the *Fshb* or *Fshr* loci may result in incomplete suppression of FSH/FSHR action in ovaries.

To date, only few TFs are known downstream of FSH signaling in ovaries including CREB and GATA 4 and 6. Our study identified additional TFs that bind FSH-regulated gene promoters (top 50 enriched shown in Fig. 3*C*, and a comprehensive list is shown in Dataset S3). Interestingly, some of these TFs themselves are regulated by FSH. Because FSHR-mediated signaling elicits multiple downstream signaling pathways in granulosa cells, we predict these signaling events must be coupled to cascades of TFs which in turn regulate target genes important for granulosa cell survival, proliferation, and differentiation. For example, we found E2F, a cell proliferation protein is FSH-activated consistent with FSH stimulation of granulosa cell proliferation (17, 19). Similarly, a well-known transcriptional repressor, REST is FSH-repressed presumably to allow granulosa cell proliferation (27–29). Our ongoing computational and future physiological studies will further identify how the network of signaling pathways–TFs–target genes are orchestrated in granulosa cells during different developmental phases.

We also found binding sites for RBPs enriched in the 3′ UTRs of FSH-regulated genes that were identified before to be physiologically important. Msi1 has been extensively studied in pituitary, mammary gland, and intestine (30–34). Together with the related family member, Msi2, Msi1 plays key roles in ovarian folliculogenesis. *Msi2* null mice display hypoplastic ovaries and impaired ovarian folliculogenesis because of preantral stage block and atresia (22). Although nothing is known about the role of PCBP1 in normal ovarian function, this RBP was identified as a tumor suppressor downregulated in ovarian cancer (35). EWSR1 is an FSH-repressed gene that preferentially targets FSH-repressed 3′ UTRs (*SI Appendix*, Fig. S3*F*). *Ewsr1* null mice are defective and display smaller ovaries that are devoid of maturing follicles and corpora lutea (36). Thus, RBPs may provide yet another layer of posttranscriptional regulation downstream of FSH signaling in granulosa cells. The identification of FSH-regulated genes/TFs along with the RBPs (based on our present study) will allow us to systematically investigate the in vivo transcriptional and posttranscriptional regulation of granulosa cell-specific gene expression in the context of overall folliculogenesis.

How FSH-regulated genes are dynamically expressed in vivo throughout the estrous cycle has never been examined. We identified six distinct patterns. All the known FSH-regulated genes fall into these patterns and provide a molecular logic for how FSH regulates estrous stages in conjunction with estrogen production and granulosa cell proliferation and differentiation. This scenario was exactly what we expected based on FSH regulation of estrogen production according to specific estrous stages (Fig. 4 *C–E*). Interestingly, we found ONECUT, a TF which is important for androgen action, is regulated by FSH. This would be physiologically relevant not to allow premature luteinization and may explain the loss of androgen conversion to estrogen by granulosa cells in the absence of FSH action.

Because our bulk RNA-seq data were generated on whole ovaries which consist of heterogenous cell populations, we further explored gene regulation at the single-cell level. Data mining from published scRNA-seq analysis on mouse ovaries (24) allowed us to capture granulosa cell–specific FSH-regulated genes and TFs that are regulated during estrous stages and were grouped into six patterns. We selected *Esr2* and *Gata6* which showed excellent correlation regarding their corresponding target genes. When ESR2 is up, the corresponding target genes go down and vice versa; similarly, when GATA6 and its targets peak in PE. Granulosa cell-specific *Gata6* knockout female mice lose FSH-responsiveness in granulosa cells with disrupted ovarian folliculogenesis (37–40). Similarly, we found that MYC, a cell cycle regulator and its targets are estrus stage specifically regulated and may drive granulosa cell proliferation as a key regulatory step downstream of FSH signaling. Collectively, our studies reveal that FSH regulates TFs and RBPs and their target genes are estrous stage specifically regulated to promote the proliferation and differentiation events in granulosa cells/ovary.

In summary, our work provides an in vivo molecular framework for future transcriptional and posttranscriptional regulation and proteomic studies downstream of FSH action in ovarian granulosa cells. The specific in vivo roles of several TFs and RBPs and their targets identified in our study can functionally be further validated by rapidly generating mutations in mice using CRISPR/CAS9 gene editing methods. These future in vivo studies may eventually allow us to identify potential targets for fertility enhancement or blockade in women.

Materials and Methods

Mice. Adult *Fshb*$^{+/+}$ and *Fshb*$^{-/-}$ mice (at 9 wk of age) were genotyped using *Fshb WT* and mutant allele-specific primers by PCR as described (6, 13). Briefly, ~1 to 2 mm mouse tail snips were protein-K digested at 56 °C for 12 to 14 h followed by DNA isolation using the Millipore DNA extraction kit. The PCR amplified DNA fragments were separated on 1.5 % agarose gels and visualized by ethidium bromide staining. All mice were on C57BL6/129SvEv hybrid genetic background and maintained on 12 h/12 h light:dark cycles in temperature and humidity-controlled rooms and water and food were provided ad libitum. All the animal procedures were approved by the University of Colorado Anschutz IACUC protocol per the NIH guidelines.

Estrous Cycle Staging. Mice were daily monitored between 9:00 am to 10:00 am for identifying diestrous, proestrous, and estrous stages from vaginal smears as described (41). Following the microscopic visualization of cellular morphology, mice were killed under isoflurane anesthesia and ovaries were harvested and either immediately placed on dry ice and stored frozen at −80 °C until further use or fixed in buffered formalin (pH 7.4) overnight at 4 °C.

Histological Analysis. Ovaries were harvested from adult (63 d) female mice under isoflurane anesthesia, immediately fixed in buffered formalin (pH 7.0) overnight at room temperature, later processed by paraffin embedding and ~6 μm thick sections were cut and stained by hematoxylin and eosin (H&E) as described (4, 6). The ovarian histology images were digitally captured by a Leica microscope and analyzed.

RNA Isolation and Library Preparation. Total RNA from mouse ovaries was obtained using RNeasy microcolumns (Qiagen), quantified by NanoDrop (ND1000) and DNase-I treated as described. RNA-Seq on ovary samples obtained from *Fshb*$^{+/+}$, *Fshb*$^{-/-}$, and *Fshb*$^{-/-}$ *HFSHB*$^{+}$ was performed at the University of Nebraska Medical Center Genomics Core and the methods were described before (42). For estrous stage study, after additional quantification by Qubit RNA assay, poly-A RNA was selected from 1,000 ng total RNA input using the New England Biolabs NEB Next Poly(A) mRNA magnetic isolation module. The isolated mRNA was further used as input for library preparation with the KAPA RNA Hyper prep kit following the manufacturer's instructions. Final libraries were quantified and quality checked using the Qubit dsDNA HS assay and Tapestation HS D1000 screentape before submitting for sequencing on the NovaSeq 6000 for 20 million 2 × 150 bp paired-end reads per library (Novogene Corp. Inc.).

RNA-Seq Analysis. Salmon (43) was used for quantifying transcript levels from all libraries using Gencode M25 transcriptome assembly (44) (parameters-l A --allowDovetail --validateMappings). All other analysis was performed in R. Briefly, Salmon data were imported using the tximport library (45). Differential gene expression was performed after filtering for expression using DESeq2 library (46) with the likelihood ratio test (Padj < 0.05). Pathway analysis was performed using GSEA (16). PWMEnrich was used to identify enrichment of non-redundant TF motifs from the JASPAR database using −1,000 bp and +250 bp from the annotated transcription start site of the most abundant transcript. PWMEnrich was also used to identify enrichment of RBP motifs using RNA bind n seq data using the 3′ UTR sequence of the most abundant transcripts.

RT-qPCR Analysis. Taqman qPCR assays on triplicate ovarian cDNA samples obtained from three genotypes of *Fshb* mice (n = 3) were performed using pre-inventoried or custom-made primer/probe combos (Integrated DNA Technologies, Inc.) as described (6, 13). The relative expression values were calculated with respect to *Ppil1* used as an internal control as described (6, 13).

Data, Materials, and Software Availability. RNA-Seq data have been uploaded to the Gene Expression Omnibus database (Accession No. GSM8288804) (47). All other data are included in the manuscript and/or supporting information.

ACKNOWLEDGMENTS. This work was supported in part by the University of Colorado Anschutz Medical Campus RNA Bioscience Initiative (N.M.), Boettcher Foundation Webb-Waring Early Career Investigator Award (N.M.), and NIH Grants GM147025 (N.M.) and HD103384, AG029531 (T.R.K.), The Makowski Family Endowment (T.R.K.), Gonadotropin Research Fund (T.R.K.), and Global Consortium on Reproductive Longevity and Equity pilot Grant-1323 (T.R.K.). K.W. is a recipient of the NSF Graduate Research Fellowship (Grant No. 1000317291).

1. P. Narayan, A. Ulloa-Aguirre, J. A. Dias, "Gonadotropins" in *Yen & Jaffe's Reproductive Endocrinology*, J. F. Strauss III, R. L. Barbieri, Eds. (Elsevier, Philadelphia, PA, ed. 8, 2019), pp. 25–57.
2. J. G. Pierce, T. F. Parsons, Glycoprotein hormones: Structure and function. *Annu. Rev. Biochem.* **50**, 465–495 (1981).
3. A. Ulloa-Aguirre, J. A. Dias, G. R. Bousfield, "Gonadotropins" in *Endocrinology of the Testis and Male Reproduction*, M. Simoni, I. Huhtaniemi, Eds. (Springer International, 2017), pp. 1–52.
4. T. R. Kumar, Y. Wang, N. Lu, M. M. Matzuk, Follicle stimulating hormone is required for ovarian follicle maturation but not male fertility. *Nat. Genet.* **15**, 201–204 (1997).
5. T. R. Kumar, M. J. Low, M. M. Matzuk, Genetic rescue of follicle-stimulating hormone beta-deficient mice. *Endocrinology* **139**, 3289–3295 (1998).
6. H. Wang *et al.*, Redirecting intracellular trafficking and the secretion pattern of FSH dramatically enhances ovarian function in mice. *Proc. Natl. Acad. Sci. U.S.A.* **111**, 5735–5740 (2014).
7. H. Wang *et al.*, Evaluation of in vivo bioactivities of recombinant hypo- (FSH(21/18)) and fully- (FSH(24)) glycosylated human FSH glycoforms in Fshb null mice. *Mol. Cell. Endocrinol.* **437**, 224–236 (2016).
8. J. S. Richards, The ovarian cycle. *Vitam. Horm.* **107**, 1–25 (2018).
9. J. S. Richards, S. A. Pangas, The ovary: Basic biology and clinical implications. *J. Clin. Invest.* **120**, 963–972 (2010).
10. Y. Arao, K. S. Korach, The physiological role of estrogen receptor functional domains. *Essays Biochem.* **65**, 867–875 (2021).
11. J. K. Findlay, S. H. Liew, E. R. Simpson, K. S. Korach, Estrogen signaling in the regulation of female reproductive functions. *Handb. Exp. Pharmacol.* **198**, 29–35 (2010).
12. S. C. Hewitt, K. S. Korach, Estrogen receptors: New directions in the new millennium. *Endocr. Rev.* **39**, 664–675 (2018).
13. H. Wang *et al.*, Identification of follicle-stimulating hormone-responsive genes in Sertoli cells during early postnatal mouse testis development. *Andrology* **11**, 860–871 (2023).
14. K. H. Burns, C. Yan, T. R. Kumar, M. M. Matzuk, Analysis of ovarian gene expression in follicle-stimulating hormone beta knockout mice. *Endocrinology* **142**, 2742–2751 (2001).
15. P. Puri *et al.*, Protein kinase A: A master kinase of granulosa cell differentiation. *Sci. Rep.* **6**, 28132 (2016).
16. A. Subramanian *et al.*, Gene set enrichment analysis: A knowledge-based approach for interpreting genome-wide expression profiles. *Proc. Natl. Acad. Sci. U.S.A.* **102**, 15545–15550 (2005).
17. J. S. Richards, From follicular development and ovulation to ovarian cancers: An unexpected journey. *Vitam. Horm.* **107**, 453–472 (2018).
18. J. S. Richards, M. Ascoli, Endocrine, paracrine, and autocrine signaling pathways that regulate ovulation. *Trends Endocrinol. Metab.* **29**, 313–325 (2018).
19. J. S. Richards, S. A. Pangas, New insights into ovarian function. *Handb. Exp. Pharmacol.* **198**, 3–27 (2010).
20. F. Gebauer, T. Schwarzl, J. Valcarcel, M. W. Hentze, RNA-binding proteins in human genetic disease. *Nat. Rev. Genet.* **22**, 185–198 (2021).
21. S. He, E. Valkov, S. Cheloufi, J. Murn, The nexus between RNA-binding proteins and their effectors. *Nat. Rev. Genet.* **24**, 276–294 (2023).
22. J. M. Sutherland *et al.*, Knockout of RNA binding protein MSI2 impairs follicle development in the mouse ovary: Characterization of MSI1 and MSI2 during folliculogenesis. *Biomolecules* **5**, 1228–1244 (2015).
23. E. Hayes, N. Winston, C. Stocco, Molecular crosstalk between insulin-like growth factors and follicle-stimulating hormone in the regulation of granulosa cell function. *Reprod. Med. Biol.* **23**, e12575 (2024).
24. M. E. Morris *et al.*, A single-cell atlas of the cycling murine ovary. *eLife* **11**, e77239 (2022).
25. T. Zhan *et al.*, A dose-response study on functional and transcriptomic effects of FSH on ex vivo mouse folliculogenesis. *Endocrinology* **165**, bqae054 (2024).
26. A. Converse *et al.*, Oocyte quality is enhanced by hypoglycosylated FSH through increased cell-to-cell interaction during mouse follicle development. *Development* **150**, dev202170 (2023).
27. A. Arizmendi-Izazaga *et al.*, The NRSF/REST transcription factor in hallmarks of cancer: From molecular mechanisms to clinical relevance. *Biochimie* **206**, 116–134 (2023).
28. L. Jin, Y. Liu, Y. Wu, Y. Huang, D. Zhang, REST is not resting: REST/NRSF in health and disease. *Biomolecules* **13**, 1477 (2023).
29. A. Nassar *et al.*, Repressor element-1 binding transcription factor (REST) as a possible epigenetic regulator of neurodegeneration and microRNA-based therapeutic strategies. *Mol. Neurobiol.* **60**, 5557–5577 (2023).
30. M. Allensworth-James *et al.*, Control of the anterior pituitary cell lineage regulator POU1F1 by the stem cell determinant Musashi. *Endocrinology* **162**, bqaa245 (2021).
31. F. M. Cambuli *et al.*, A mouse model of targeted Musashi1 expression in whole intestinal epithelium suggests regulatory roles in cell cycle and stemness. *Stem Cells* **33**, 3621–3634 (2015).
32. R. I. Glazer, D. T. Vo, L. O. Penalva, Musashi1: An RBP with versatile functions in normal and cancer stem cells. *Front. Biosci. (Landmark Ed.)* **17**, 54–64 (2012).
33. A. K. Odle *et al.*, Association of Gnrhr mRNA with the stem cell determinant Musashi: A mechanism for leptin-mediated modulation of GnRHR expression. *Endocrinology* **159**, 883–894 (2018).
34. Y. Song *et al.*, The Msi1-mTOR pathway drives the pathogenesis of mammary and extramammary Paget's disease. *Cell Res.* **30**, 854–872 (2020).
35. W. Zhang *et al.*, Poly C binding protein 1 regulates p62/SQSTM1 mRNA stability and autophagic degradation to repress tumor progression. *Front. Genet.* **11**, 930 (2020).
36. H. Li *et al.*, Ewing sarcoma gene EWS is essential for meiosis and B lymphocyte development. *J. Clin. Invest.* **117**, 1314–1323 (2007).
37. J. Bennett, S. C. Baumgarten, C. Stocco, GATA4 and GATA6 silencing in ovarian granulosa cells affects levels of mRNAs involved in steroidogenesis, extracellular structure organization, IGF-I activity, and apoptosis. *Endocrinology* **154**, 4845–4858 (2013).
38. J. Bennett, Y. G. Wu, J. Gossen, P. Zhou, C. Stocco, Loss of GATA-6 and GATA-4 in granulosa cells blocks folliculogenesis, ovulation, and follicle stimulating hormone receptor expression leading to female infertility. *Endocrinology* **153**, 2474–2485 (2012).
39. J. Bennett-Toomey, C. Stocco, GATA regulation and function during the ovarian life cycle. *Vitam. Horm.* **107**, 193–225 (2018).
40. M. Heikinheimo *et al.*, Expression and hormonal regulation of transcription factors GATA-4 and GATA-6 in the mouse ovary. *Endocrinology* **138**, 3505–3514 (1997).
41. R. Behringer, M. Gertsenstein, K. V. Nagy, A. Nagy, Selecting female mice in estrus and checking plugs. *Cold Spring Harb. Protoc.* 2016, 8 (2016).
42. R. McDonald *et al.*, RNA-seq analysis identifies age-dependent changes in expression of mRNAs–Encoding N-glycosylation pathway enzymes in mouse gonadotropes. *Mol. Cell Endocrinol.* **574**, 111971 (2023).
43. R. Patro, G. Duggal, M. I. Love, R. A. Irizarry, C. Kingsford, Salmon provides fast and bias-aware quantification of transcript expression. *Nat. Methods* **14**, 417–419 (2017).
44. A. Frankish *et al.*, Gencode 2021. *Nucleic Acids Res.* **49**, D916–D923 (2021).
45. C. Soneson, M. I. Love, M. D. Robinson, Differential analyses for RNA-seq: Transcript-level estimates improve gene-level inferences. *F1000Res* **4**, 1521 (2015).
46. M. I. Love, W. Huber, S. Anders, Moderated estimation of fold change and dispersion for RNA-seq data with DESeq2. *Genome Biol.* **15**, 550 (2014).
47. K. Walters *et al.*, Discovery of FSH-regulated and estrus stage-specific transcriptional networks in mouse ovaries. Gene Expression Omnibus. https://www.ncbi.xyz/geo/query/acc.cgi?acc=GSM8288804. Deposited 23 May 2024.